Assessing Annual Risk of Vehicles Hit by a Rainfall Induced Landslide: A Case Study on Kennedy Road in Wan Chai, Hong Kong

Meng Lu[1], Jie Zhang[2*], Lulu Zhang[3] and Limin Zhang[4]

Abstract: Landslides threaten the safety of vehicles on highways. In analyzing the risk of landslide hitting the moving vehicles, the spacing between vehicles and the type of vehicles on the highway could be highly uncertain, which are often not considered in previous studies. Through a case study about a highway slope in Hong Kong, this paper presents a method to assess the risk of moving vehicles hit by a rainfall-induced landslide, in which the possible number of different types of vehicles being hit by the landslide can be investigated. In this case study, the annual failure probability of the slope is analyzed based on historical slope failure data in Hong Kong. The spatial impact of the landslide is evaluated based on an empirical runout prediction model. The consequence is assessed through probabilistic modeling of the traffic, which can consider uncertainties of vehicles spacing, vehicle types and slope failure time. With the suggested method, the expected annual number of vehicles and persons being hit by the landslide can be conveniently calculated. It can also be used to derive the cumulative frequency-number of fatalities curve for societal risk assessment. With the suggested method, the effect of factors like the annual failure probability of the slope and the density of vehicles on the risk of the slope can be conveniently assessed. The method described in this paper can provide a new guideline for highway slope design in terms of managing the risk of landslide hitting moving vehicles.

Key words: Risk assessment; Uncertainty; Landslide; Hit; Vehicles

[1] Research Assistant, Key Laboratory of Geotechnical and Underground Engineering of Ministry of Education and Department of Geotechnical Engineering, Tongji University, Shanghai 200092, China. E-mail: lumeng@tongji.edu.cn
[2] Professor, Key Laboratory of Geotechnical and Underground Engineering of Ministry of Education and Department of Geotechnical Engineering, Tongji University, Shanghai 200092, China. E-mail: cezhangjie@tongji.edu.cn
[3] Professor, State Key Laboratory of Ocean Engineering and Department of Civil Engineering, Shanghai Jiao Tong University, Shanghai 200240, China. E-mail: lulu_zhang@sjtu.edu.cn
[4] Professor, Department of Civil Engineering, Hong Kong University of Science and Technology, Clear Water Bay, Hong Kong, China. E-mail: cezhangl@ust.hk

1 Introduction

With a total land area of about 1100 km^2, Hong Kong is one of the most densely populated regions in the world with a population of about 7.5 million (GovHK, 2019). Throughout the territory of Hong Kong, there are more than 57, 000 registered man-made slope features (Cheung and Tang, 2005). With an average annual rainfall of about 2400 mm, rainfall induced landslides are one of the major natural hazards threatening the public safety in Hong Kong (GEO, 2017). In particular, slope failures along highways have resulted in serious fatalities and damaged vehicles. For example, in August 1994, a public light bus on the Castle Peak Road was hit by landslide debris, causing three persons trapped inside the bus and one man killed. In August 1995, due to the intense rainfall, the landslide along Shum Wan Road resulted in two fatalities and five injuries, and the landslide along Fei Tsui Road resulted in one fatality and one injury (GEO, 2017). Similar phenomena has indeed also been reported in many other parts of the world (Bil et al., 2015), such as Italy (Donnini et al., 2017) and India (Negi et al., 2013).

There are many uncertainties in the assessment of the hazard of moving vehicles hit by a landslide, such as the occurrence of the landslide, the spatial impact of the landslide, the number of vehicles being hit by the landslide, and the type of vehicles being hit by the landslide. Risk assessment is a framework in which both the uncertainties and the consequence of a hazard can be addressed, which has now increasingly been used for landslide risk management (e.g. Lessing et al., 1983; Fell, 1994; Dai et al., 2002; Remondo et al., 2008; Erener, 2012; Vega and Hidalgo, 2016). Indeed, landslide risk assessment has been accepted as an effective tool for the planning of land use in Hong Kong. Nevertheless, the risk assessment of moving vehicles affected by landslides is special because the elements at risk are highly mobile. Previously, many studies have been conducted to study the individual risk associated with the landslide, which is often measured by that the annual probability

47 that a person who frequently uses the highway was killed by the landslide (e.g. Bunce et al., 1997; Fell
48 et al., 2005; Dorren et al., 2009; Michoud et al., 2012; Macciotta et al., 2015; Macciotta et al., 2017).
49 Several studies have also examined the societal risk of vehicles being hit be landslides, in which the
50 societal risk is measured in terms of the annual probability that at least one fatality occurs in one year
51 (e.g. Budetta, 2004; Peila and Guardini, 2008; Pierson, 2012; Ferlisi et al., 2012; Corominas et al.,
52 2013; Macciotta et al., 2019). These studies have provided both useful insights and practical tools for
53 analysis and management of the landslide/rockfall hazards. Nevertheless, it was commonly assumed
54 that the traffic is uniformly distributed in time and space, and that each vehicle had the mean length of
55 all vehicles (e.g. Hungr et al., 1999; Nicolet et al., 2016). In reality, there is randomness associated
56 with the spacing among vehicles on the highway. If such uncertainties are ignored, the resulting
57 uncertainty associated with the number of vehicles being hit by the landslide cannot be considered in
58 the risk assessment process. Also, there might be multiple types of vehicles on the highway, and
59 different types of vehicles may have different lengths and also significant different passenger
60 capacities. If the difference between different types of vehicles is ignored, it might be hard to estimate
61 the number of people being hit by the landslide, which is also an important aspect of risk assessment.
62 Through a case study on Kennedy Road in Wan Chai, Hong Kong, this paper aims to suggest a
63 new method to assess the risk of moving vehicles hit by a rainfall-induced landslide, in which the
64 possible number of different types of vehicles being hit by the landslide can be investigated. In general,
65 quantitative analysis of vehicles endangered by landslides includes three scenarios, i.e., (1) a moving
66 vehicle is impacted by falling materials, (2) a moving vehicle impacts falling materials on highway,
67 and (3) a line of stationary vehicles is impacted by falling materials (Bunce et al., 1997). In this study,
68 our focus is on the risk assessment of moving vehicles impacted by a falling landslide. The structure

of this paper is as follows. Firstly, the annual failure probability of the slope is calculated based on historical data in Hong Kong. Then, the spatial impact of the landslide is analyzed based on the runout distance analysis. Thereafter, the consequence of the landslide is analyzed via a probabilistic model of traffic. Finally, the annual expected numbers of vehicles and persons being hit by the landslide are calculated, and how it can be used to develop the F-N curve for societal risk assessment is also illustrated. Factors affecting the risk of vehicles hit by the landslide are also discussed. The method suggested in this paper can support establishing new guidelines for highways design for purposes of roadway safety in terms of landslide risk reduction hitting vehicles and persons.

2 Study Slope and Traffic Information

The study slope is located on Kennedy Road in Wan Chai district of Hong Kong as shown in Fig. 1. Wan Chai is one of the most traditional cultural areas in Hong Kong and attracts many tourists around the world every year. In addition, Kennedy Road is a major road with three lanes in this area, linking with the Queen's Road in Wan Chai (TDHK, 2018). On 8 May 1992, the slope failed during an intense rainfall, which hit a car travelling along Kennedy Road and killed the driver (GEO, 1996). The slope is an old cut slope formed in 1967 and 1968, which was covered by trees before the occurred landslide event. Fig. 2 shows a typical cross section of the slope and the occurred landslide event. As shown in this figure, the rainfall infiltration triggered the failure of the soil mass below the retaining wall and the sliding mass hit the vehicle. The height of the slope, H, is 25 m. The horizontal distance from the crest of the landslide scar to the side of Kennedy Road close to the slope, l_{ch}, is 35 m and the horizontal distance from the slope toe to the side of Kennedy Road close to the slope, l_{th}, is 3 m. The width of Kennedy Road, b_h, is 10 m. Fig. 3 shows the plan view of the occurred landslide event. The width of

91 the slope is 18 m and the volume of the landslide is 500 m^3 (GEO, 1996). According to Transport
92 Department of Hong Kong (TDHK) (2018), vehicles in Hong Kong are composed of private buses,
93 non-franchised public buses, franchised buses, taxis, private cars, public light buses, private light buses,
94 goods vehicles, special purpose vehicles, government vehicles and motor cycles. The percentage of
95 each type of vehicle with respect to total numbers of vehicles is shown in Table 1 (TDHK, 2018).
96 Additionally, the typical length of each type of vehicle and the passenger capacity of each type of
97 vehicle are also shown in Table 1 (TDHK, 2018). The purpose of this case study is to analyze the
98 annual risk of different types of vehicles hit by the landslide if the slope fails again due to rainfall.
99

100 ## 3 Methodology

101 There are multiple types of vehicles on a highway. In a landslide critical zone of the road, the longer
102 the vehicle, the greater the probability that it will be hit by a landslide. Fig. 4 shows the event tree
103 model employed in this study to assess the risk of rainfall-induced landslide hitting type *j* vehicles. As
104 can be seen from this figure, if the slope does not fail in a year, there will be not spatial impact, and
105 the number of type *j* vehicles being hit is zero. Let $P(F)$ denote the annual probability of slope failure.
106 If the slope fails, its spatial impact, which can be characterized by the width of the landslide mass and
107 the runout distance of the landslide mass, is also uncertain. In general, the spatial impact of the
108 landslide depends on factors like slope geometry, soil profile, soil strength parameters, and water
109 content in the soil mass. The spatial impact can be evaluated using physically-based methods or
110 statistically-based methods, and will be discussed later in this paper. Suppose there are *m* possible
111 spatial impacts and let $P(\mathbf{S} = \mathbf{S}_i | F)$ denote the probability that the spatial impact is $\mathbf{S}_i$ when the landslide
112 occurs. For a given spatial impact, the number of type *j* vehicles being hit is also uncertain. Let n_j

denote the number of the type j vehicle being hit by the landslide. Let $P(n_j = k|\ \mathbf{S} = \mathbf{S}_i)$ denote the encounter probability that k type j vehicles will be hit by the landslide when the spatial impact is $\mathbf{S}_i$. If the landslide mass cannot reach the road for the case of $\mathbf{S} = \mathbf{S}_i$, the spatial impact is zero, which can be denoted as $P(n_j = 0|\ \mathbf{S} = \mathbf{S}_i) = 1$.

Based on the event tree as shown in Fig. 4, the annual probability of k type j vehicles being hit by the landslide is $P(F) \times P(\mathbf{S} = \mathbf{S}_i|\ F) \times P(n_j = k|\ \mathbf{S} = \mathbf{S}_i)$ when the spatial impact of the landslide is $\mathbf{S}_i$, and expected number of type j vehicles being hit corresponding to such a scenario is $k \times P(F) \times P(\mathbf{S} = \mathbf{S}_i|\ F) \times P(n_j = k|\ \mathbf{S} = \mathbf{S}_i)$. As the pathways are mutually exclusive, the annual expected number of type j vehicles being hit by the landslide, E_{vj}, is the summation of expected numbers corresponding to all the pathways in Fig. 4, which can be written as follows:

$$E_{vj} = P\left(F\right) \times \sum_{i=1}^{m} \left[P\left(\mathbf{S} = \mathbf{S}_i \mid F\right) \times \sum_{k=0}^{\infty} kP\left(n_j = k \mid \mathbf{S} = \mathbf{S}_i\right) \right] \tag{1}$$

Let n denote total types of vehicles. The total expected number of vehicles being hit by the landslide considering all types of vehicles, i.e., E_v, can then be calculated as follows:

$$E_v = \sum_{j=1}^{n} E_{vj} \tag{2}$$

Let n_{pj} denote the passenger capacity in a type j vehicle. The expected number of people in type j vehicles being hit by the landslide, E_{pj}, can be calculated as follows:

$$E_{pj} = P\left(F\right) \times \sum_{i=1}^{m} \left[P\left(\mathbf{S} = \mathbf{S}_i \mid F\right) \times \sum_{k=0}^{\infty} kP\left(n_j = k \mid \mathbf{S} = \mathbf{S}_i\right) \right] \times n_{pj} \tag{3}$$

The total expected number of people being hit by the landslide considering all types of vehicles, E_p, can be calculated as follows:

$$E_p = \sum_{j=1}^{n} E_{pj} \tag{4}$$

Eq. (2) can be extended to estimate the expected monetary losses of vehicles being hit by a landslide when information regarding the price of different types of vehicles is available. Nevertheless, during the analysis of the risk of vehicles hit by landslides, the social impact, which can be better measured by the number of vehicles than the cost of the vehicles, is often more important than the economic losses. Hence, the risk of vehicles hit by landslides is not measured in terms of monetary losses in this study.

Previously, the individual risk is often used to measure the threat of a landslide to a moving vehicle, which provides information about the probability of a frequent user of the highway to be killed by the landslide. On the other hand, decision makers may also be interested in the annual expected numbers of vehicles/persons being hit by the landslide, which can be obtained using the method suggested in this paper. As will be shown later in the case study, the above framework can be easily extended to calculate the F-N curve for societal risk assessment, which is an important complement to previous methods on social risk assessment relying solely on the probability of at least one fatality per year.

As indicated by Eq. (1), the keys for the annual risk associated with the type j vehicle are to evaluate: (1) the annual failure probability of the landslide, i.e., $P(F)$, (2) the possible spatial impact of the landslide, i.e., $P(\mathbf{S} = \mathbf{S}_i | F)$ and (3) the encounter probability that possible number of the type j vehicle being hit by the landslide for a given spatial impact, i.e., $P(n_j = k | \mathbf{S} = \mathbf{S}_i)$. How the above elements are assessed will be introduced in the following sections.

3.1 Evaluation of annual probability of the landslide, $P(F)$

154 The estimation of annual landslide probability or landslide susceptibility is fundamental in landslide
155 hazard assessment. Since almost slope failures in Hong Kong are caused by rainfall infiltration (e.g.
156 Lumb, 1975; Brand, 1984; Finlay et al., 1999), assessing annual probability of rainfall-induced
157 landslides is important. In general, there are two types of methods for evaluating the likelihood of slope
158 failure, i.e., physically based methods through slope stability analysis (e.g. Christian et al., 1994;
159 Fenton and Griffiths, 2005; Huang et al., 2010) and empirical methods through statistical analysis of
160 historical slope failure data (e.g. Chau et al., 2004; Tang and Zhang, 2009). Currently, landslide
161 probability analyses via slope stability analyses mainly focus on the likelihood of slope failure for a
162 given rainfall. In reality, the occurrence of landslides in a year is highly uncertain. Currently, how to
163 calculate the annual failure probability of a landslide using physically-based models considering
164 rainfall uncertainty is still not well established. Hence, the statistical methods are adopted in this study
165 to estimate the annual landslide probability.

166 In Hong Kong, the failure of a slope is highly correlated to the 24-hour rainfall, i_{24} (Cheung and
167 Tang, 2005). Based on i_{24}, the rainstorms in Hong Kong can be divided into three categories, i.e., (1)
168 $i_{24} < 200$ mm/day (small rainfall, denoted as *SR*), (2) 200 mm $< i_{24} <$ 400 mm/day (medium rainfall,
169 denoted as *MR*) and (3) $i_{24} > 400$ mm/day (large rainfall, denoted as *LR*) (Zhang and Tang 2009).
170 Through statistical analysis of the slope failure data in Hong Kong during 1984-2002, it is found that
171 the failure probability of a slope in Hong Kong when subjected to small rainfall, medium rainfall and
172 large rainfall are 1.09×10^{-4}, 2.61×10^{-3} and 8.94×10^{-3}, respectively, i.e., $P(F|\,SR) = 1.09 \times 10^{-4}$, $P(F|$
173 $MR) = 2.61 \times 10^{-3}$ and $P(F|\,LR) = 8.94 \times 10^{-3}$ (Zhang and Tang, 2009). In the statistical analysis, it is
174 assumed that slopes in Hong Kong when subjected to the same type of rainfall have the same failure
175 probability, and hence the failure probability obtained should be interpreted as the failure probability

of an average slope. Such an assumption is commonly adopted in statistically-based method for evaluating the failure probability of slopes in a region. As noticed by Dai et al. (2002), such a method cannot consider the effect of local geology and soil condition on the site-specific slope stability.

In Zhang and Tang (2009), the conditional failure probability of a slope for a given type of rainfall is provided. To calculate the annual failure probability of a slope, the uncertainty associated with the rainfall should be analyzed. In this study, the uncertainty associated with rainfall can be represented by the uncertainty associated with i_{24}. To characterize the uncertainty associated with i_{24}, we collected yearly maximum i_{24} measured at Hong Kong Observatory Headquarters during 1969 and 2018 as shown in Figure 5 (HKO, 2018). As can be seen from Fig. 5, the maximum i_{24} in a year in Hong Kong is mainly in the range of 100 to 350 mm. The generalized extreme value distribution (Hosking et al., 1985) with the following probability density function (PDF) seems to fit the histogram with reasonable accuracy:

$$f\left(i_{24}\right) = \frac{1}{\beta}\left[1 + \gamma\left(\frac{i_{24} - \mu}{\beta}\right)\right]^{-\frac{1}{\gamma}} \exp\left\{\left[1 + \gamma\left(\frac{i_{24} - \mu}{\beta}\right)\right]^{-\frac{1}{\gamma}}\right\} \quad (5)$$

where β, μ and γ are the scale parameter, the location parameter and the shape parameter of the generalized extreme distribution, respectively. The values of β, μ and γ can be calculated based on maximum likelihood method and they are equal to -0.17, 66 and 188, respectively. Fig. 6 shows the cumulative distribution function (CDF) of i_{24} obtained based on the fitted generalized extreme value distribution. As can be seen from this figure, the probability that the rainfall with yearly maximum i_{24} belongs to small rainfall, medium rainfall and large rainfall is 0.44, 0.55 and 0.01, respectively, i.e., $P(SR) = 0.44$, $P(MR) = 0.55$ and $P(LR) = 0.01$. Based on the total probability theorem, the annual probability of a rainfall induced slope failure can be computed as follows:

$$P\left(F\right) = P\left(F \mid SR\right)P\left(SR\right) + P\left(F \mid MR\right)P\left(MR\right) + P\left(F \mid LR\right)P\left(LR\right) \quad (6)$$

With the above equation, the impact of uncertainty of rainfall on the annual failure probability of the landslide is considered. The failure probability obtained is unconditional on the rainfall type and hence does not correspond to a certain return period of rainfall.

3.2 Evaluation of spatial impact of the landslide, $P(\mathbf{S} = \mathbf{S}_i \mid F)$

In this study, the spatial impact of the landslide is characterized by the landslide width and the runout distance of the landslide. Let b_l denote the width of the landslide. Let L denote the runout distance of the landslide, which is defined as the distance between the crest of the landslide scar and the toe of the slip. Thus, $\mathbf{S} = \{b_l, L\}$. For simplicity, the uncertainty of the landslide width is not considered. In such a case, the uncertainty associated with $\mathbf{S}$ is fully characterized by the uncertainty associated with the runout distance. In principle, the runout distance is a continuous random variable. For ease of computation, it can be discretized into a discrete variable. Let L_i denote the ith possible value of L. Then, $P(\mathbf{S} = \mathbf{S}_i \mid F)$ can be calculated by

$$P\left(\mathbf{S} = \mathbf{S}_i \mid F\right) = P\left(L = L_i\right) \quad (7)$$

In general, the runout distance of a landslide depends on factors like the slope geometry, the soil profile, and geotechnical, hydraulic and rheological properties of sliding mass. The methods to investigate the runout distance of a landslide can be divided into two categories (Hungr et al., 2005): (1) analytical or numerical methods based on the physical laws of solid and fluid dynamics (Scheidegger, 1973), which are usually solved numerically (e.g. Hungr and McDougall, 2009; Luo et al., 2019) and (2) empirical methods based on field observations and geometric correlations (e.g. Dai and Lee, 2002; Budetta and Riso, 2004). The use of the physically-based methods require detailed

information on the ground condition as well as the geotechnical and hydraulic properties of the soils. On the other hand, empirical methods based on geometry of the landslide are generally simple and relatively easy to use (e.g. Finlay et al., 1999; Dai et al., 2002). In this study, the empirical method is adopted due to lack of information of geotechnical and hydraulic conditions of the slope. In particular, the following empirical equation is used (Corominas, 1996):

$$\log L = 0.085 \log V + \log H + 0.047 + \varepsilon \quad (8)$$

where V is the volume of the sliding mass and H is the height of the slope; ε is a random variable with a mean of zero and a standard deviation of $\sigma = 0.161$. As shown in Finlay et al. (1999) and Gao et al. (2017), Eq. (8) can predict the runout distance of cut and fill slopes in Hong Kong quite well. As mentioned previously, the slope studied in this paper is indeed a cut slope.

For the slope as shown in Fig. 2, the height is 25 m, i.e., $H = 25$ m. To apply Eq. (8), the landslide volume is needed. In general, the volume of a landslide can be estimated through methods based on surface-area volume relationship (e.g. Malamud et al., 2004; Imaizumi and Sidle, 2007; Guzzetti et al., 2008; Guzzetti et al., 2009), slope stability analysis (e.g. Huang et al., 2013; Chen and Zhang, 2014), or morphology-based methods (e.g. Carter and Bentley, 1985; Jaboyedoff et al., 2012). A comprehensive review of such methods can be found in Jaboyedoff et al. (2020). With these methods, the volume of a sliding mass can be estimated both for a slope that has not failed yet and for a landslide that has occurred. In this study, the volume is estimated through the surface-area volume relationship. Let A_s denote the landslide scar area. The volume of the landslide in this case study is estimated with A_s using the following equation (Parker 2011):

$$V = 0.106 \times A_s^{1.388} \quad (9)$$

240 Based on Fig. 3, the landslide scar area is estimated to be 450 m^2. Based on Eq. (9), the volume
241 is estimated about 510 m^3, which is close to the volume of sliding mass (500 m^3) reported in GEO
242 (1996). Substituting the values of H and V into Eq. (8), it can be obtained that the travel distance of the
243 landslide is lognormally distributed with a mean of 50.7 m and a standard deviation of 12.6 m. Fig. 7
244 shows the PDF of the travel distance of the landslide. As can be seen from this figure, the travel distance
245 of the landslide is mainly in the range of 20 m to 150 m.
246
247 ### 3.3 Evaluation of encounter probability, $P(n_j = k | \mathbf{S} = \mathbf{S}_i)$
248 As shown in Fig. 2, the horizontal distance from the crest of the landslide scar to the side of Kennedy
249 Road close to the slope (l_{ch}) is 35 m. The width of Kennedy Road (b_h) is 10 m. When $L_i > l_{ch}$, the
250 landslide will reach Kennedy Road. When $L_i \geq l_{ch} + b_h$, the Kennedy Road will be totally covered by
251 the sliding mass. When $l_{ch} < L_i < l_{ch} + b_h$, the Kennedy Road will be partially affected. Thus, the percent
252 of vehicles within the affected length of the highway for a given spatial impact, denoted as $\alpha(\mathbf{S} = \mathbf{S}_i)$
253 here, can be calculated as follows:
254
$$\alpha\left(\mathbf{S}=\mathbf{S}_i\right)=\begin{cases}0, & L_i \leq l_{ch} \\ \dfrac{L_i - l_{ch}}{b_h}, & l_{ch} < L_i < l_{ch} + b_h \\ 1, & L_i \geq l_{ch} + b_h\end{cases} \tag{10}$$

255 $\alpha(\mathbf{S} = \mathbf{S}_i)$ can also be interpreted as the degree of affection related to the runout distance. As can
256 be seen from Eq. (10), $\alpha(\mathbf{S} = \mathbf{S}_i)$ is between 0 (the sliding mass does not reach the road) and 1 (the
257 sliding mass totally covers the road). For a given runout distance, the number of vehicles hit by the
258 landslide highly depends on the length of road affected by the landslide as well as the density of
259 vehicles. Let l_a denote the length of road affected by the landslide. Let l_v denote the length of vehicles.
260 As shown in Fig. 3, when the head or the rear of a vehicle contacts with the landslide mass, the vehicle

will be hit by the landslide, i.e., the length of affected road, l_a, is equal to the sum of the width of the landslide (b_l) and the length of the vehicles (l_v) as follows:

$$l_a = b_l + 2l_v \tag{11}$$

In this study, the width of the landslide is assumed to equal to the width of the slope, i.e., $b_l = 18$ m (GEO, 1996). In transportation, the presence of the vehicles on a highway can be modeled as a Poisson process with a mean arrival rate of λ, which is equal to the density of vehicles on a highway (Paxson and Floyd, 1995). Let q denote the number of vehicles passing a given cross section of a road per unit time. Let v denote the average speed of the vehicles. The mean rate of occurrence of moving vehicles (λ) can be calculated as follows (Lighthill, 1995):

$$\lambda = \frac{q}{v} \tag{12}$$

Let w_j denote the proportion of type j vehicle in the traffic flow. The mean rate of occurrence of type j vehicles can be then written as follows:

$$\lambda_j = w_j \times \frac{q}{v} \tag{13}$$

In general, the presence of vehicles also depends on the periods in a day. As an example, Table 2 shows the data about q and v of the Kennedy road for the morning peak, normal period and evening peak, respectively (TDHK 2018). Then, the mean rate of occurrence of each type of vehicle is obtained for different periods of a day, as shown in Figs. 8(a)–(c), respectively. It can be seen that the mean rate of occurrence of the vehicles during the morning and evening peaks is significantly larger than that in the normal period. Among all types of vehicles, the mean rate of private cars in the affected road is the greatest, followed by goods vehicles, motor cycles and taxis.

Let T_1, T_2 and T_3 denote the morning peak, the normal period and the evening peak, respectively, and let l_{aj} denote the length of affected road for type j vehicle. Based on the property of a Poisson process, if the spatial impact is $\mathbf{S}_i$ and the slope fails during period T_i, the encounter probability that k type j vehicles will be hit by the landslide can be computed by

$$P\left(n_j = k \mid t \in T_i, \mathbf{S} = \mathbf{S}_i\right) = \frac{\left[\alpha_j \left(\mathbf{S} = \mathbf{S}_i\right) \lambda_j l_{aj}\right]^k}{k!} \exp\left[-\alpha_j \left(\mathbf{S} = \mathbf{S}_i\right) \lambda_j l_{aj}\right] \tag{14}$$

Eq. (14) provides a probabilistic model of the number of vehicles hit by the landslide, which can consider uncertainties of vehicles spacing, vehicle types and slope failure time. As an example, Figs. 9(a)–(c) show the probability distributions of the number of private cars being hit by the landslide during the morning peak, normal period and evening peak when the spatial impact is $\mathbf{S}_i$ and $\alpha_j(\mathbf{S} = \mathbf{S}_i) = 1$, respectively. As can be seen from these figures, the most probable number of private cars being hit by the landslide during the morning peak and evening peak is both about 3 and its probability is both about 0.20. The most probable number of private cars being hit by the landslide during the normal period is about 1 and its probability is about 0.37.

In reality, the slope can fail during any period of a day. Based on the total probability theorem, the probability that k type j vehicles will be hit for the case of $\mathbf{S} = \mathbf{S}_i$ can be computed by

$$P\left(n_j = k \mid \mathbf{S} = \mathbf{S}_i\right) = \sum_{i=1}^{3} P\left(n_j = k \mid t \in T_i, \mathbf{S} = \mathbf{S}_i\right) P\left(t \in T_i\right) \tag{15}$$

As an example, Figs. 9(d) shows the probability distribution of the number of private cars being hit by the landslide considering the uncertainty of the failure time when the spatial impact is $\mathbf{S}_i$ and $\alpha_j(\mathbf{S} = \mathbf{S}_i) = 1$. As can be seen from this figure, the most probable number of private cars hit by the landslide considering the uncertainty of the failure time is about 1 and its probability is about 0.32.

3.4 Risk calculation and evaluation

In the above analyses, equations for evaluating $P(F)$, $P(\mathbf{S} = \mathbf{S}_i | F)$ and $P(n_j = k | \mathbf{S} = \mathbf{S}_i)$ are introduced. Substituting these equations into Eq. (1), the expected number of each type of vehicles being hit by the landslide can then be calculated, as shown in Figs. 10(a). As can be seen from this figure, the expected number of private cars being hit by the landslide is the greatest with a value of 1.67×10^{-3} vehicles per year, followed by the goods vehicles, motor cycles and taxis. The expected number of each type of vehicles being hit by the landslide is highly correlated with the proportion of vehicles in the traffic flow. The private cars have the greatest proportion in the traffic flow and hence it is natural to be associated with the greatest expected number. In reality, the vehicle that was hit by the studied slope on 8 May 1992 was indeed a private car. With Eq. (2), the total expected number of vehicles being hit by the landslide considering all types of vehicles can be also calculated, which is about 2.48×10^{-3} vehicles per year.

Submitting the passenger capacity of each type of vehicle into Eq. (3), the expected number of persons being hit by the landslide associated with each type of vehicle can be computed and the results are shown in Figs. 10(b). As can be seen from this figure, the expected number of persons being hit by the landslide for private cars is the greatest with a value of 8.37×10^{-3} persons per year, followed by non-franchised public buses, franchised buses and goods vehicles. The expected number of persons being hit by the landslide for each type of vehicles highly depends on the proportion of vehicles in the traffic flow and the passenger capacity of vehicles. The non-franchised public buses have the higher proportion in the traffic flow and the largest passenger capacity hence it is natural to be associated with the greater expected number. Based on Eq. (4), the total expected number of persons being hit by the

323 landslide considering all types of vehicles can be also calculated, which is about 1.36×10^{-2} persons
324 per year.

325 The society is less tolerant of events in which a large number of lives are lost in a single event,
326 than of the same number of lives are lost in a large number of separate events, which can be measured
327 through societal risk (Cascini et al., 2008). In Hong Kong, the societal risk is measured through F-N
328 relationship (GEO, 1998), as shown in Fig. 11. In this figure, the horizontal axis denotes the number
329 of fatalities, and the vertical axis denotes cumulative annual frequency of the number of fatalities.
330 There are four regions in this figure, i.e., the region in which the risk is unacceptable, the region in
331 which the risk is broadly acceptable, the region in which the risk should be made as low as reasonably
332 practicable (ALARP), and the intense scrutiny region. To assess the societal risk of the landslide, the
333 relationship between the number of fatalities and the probability of such an event should be established.
334 When the traffic flow is a Poisson process, the passengers in the traffic flow can also be modeled
335 through Poisson process. For example, the mean rate of occurrence of passengers in type j vehicle is
336 $\lambda_{pj} = n_{pj}\lambda_j$ where n_{pj} is the passenger capacity of type j vehicles and λ_j is the mean rate of occurrence of
337 type j vehicles. Let n_{jp} denote the number of people being hit by the landslide. Using equations similar
338 to Eqs. (14) and (15), the chance of k passengers in type j vehicles hit by the landslide for a given
339 spatial impact can also be calculated, which is denoted as $P(n_{jp} = k | \mathbf{S} = \mathbf{S}_i)$. The annual chance of k
340 passengers in type j vehicles being hit by the landslide can be calculated as:

341 $$P\left(n_{jp} = k\right) = P(F)\sum_{i=1}^{m}\left[P\left(n_{jp} = k \mid \mathbf{S} = \mathbf{S}_i\right)P\left(\mathbf{S} = \mathbf{S}_i \mid F\right)\right] \quad (16)$$

342 Fig. 11 shows the relationships between the number of people being hit by the landslide and the
343 annual probability such an event occurs for different types of vehicles. As can be seen from this figure,
344 the risk associated with type 5 vehicles (private cars) is greatest and unacceptable. The risk associated

345 with type 1 vehicles (private buses), type 9 vehicles (special purpose vehicles), and type 10 vehicles
346 (government vehicles) are in the acceptable region. The risk associated with the rest types of vehicles
347 are in the ALARP region. Indeed, the people being hit by the landslide on 8 May 1992 was a person in
348 the private car.

349 As the flow of all vehicles on the highway is modeled as a Poisson process, the flow of people on
350 the highway considering all types of vehicles can also be modeled as Poisson process with a mean rate
351 of $\lambda_p = \lambda(w_1 n_{p1} + w_2 n_{p2} + \ldots w_n n_{pn})$ where w is the proportion of each type of vehicle in the traffic flow,
352 n is the number of vehicle types and λ is the mean rate of occurrence of all vehicles. Using an equation
353 similar to Eq. (16), the annual probability of k persons in the traffic flow considering all types of
354 vehicles can also be calculated, and the obtained F-N curve considering all types of vehicles is also
355 shown in Fig. 11. As can be seen from this figure, the social risk considering all types of vehicles is
356 greater than that of any individual type of vehicles and hence is also unacceptable.

357

358 ## 4 Discussions

359 ### 4.1 Effect of annual failure probability of the slope

360 In the above analysis, the annual failure probability of the slope only represents the failure probability
361 of an average slope in Hong Kong. To investigate the effect of the failure probability of the slope, Fig.
362 12 shows the how the annual expected number of vehicles and people being hit by the landslide for all
363 types of vehicles changes with the annual failure probability of the slope. As can be seen from this
364 figure, the expected number of vehicles hit by the landslide increases linearly as the annual failure
365 probability of the slope increases. When the failure probability of the slope increase from 1.0×10^{-4} to
366 1.0×10^{-2}, the expected number increases from 1.57×10^{-4} vehicles being hit per year to 1.57×10^{-2}

367 vehicles being hit per year. A similar observation can also be found for the annual expected number of
368 persons being hit by the landslide. Fig. 13 shows the how the societal risk for all types of vehicles
369 changes as the annual failure probability of the slope changes. As can be seen from this figure, when
370 the failure probability of the slope is smaller than 1.0×10^{-4}, the societal risk will be in the ALARP
371 region. If the failure probability of the slope is further reduced to 1.0×10^{-6}, the societal risk will
372 become acceptable. Hence, reducing the annual failure probability of a slope is an effective means to
373 reduce the risk of the slope. In practice, the annual failure probability of a slope under rainfall can be
374 reduced through the use of engineering measures such as structural reinforcement. To assess the effect
375 of such measures on the failure probability of the slope, physically-based methods shall be used for
376 hazard probability analysis.
377
378 ## 4.2 Effect of traffic density
379 The density of vehicles may vary from one road to another. To investigate the effect of density of
380 vehicles, the annual expected number of vehicles and people being hit by the landslide and the annual
381 societal risk for all types of vehicles are investigated when the density of vehicles on the highway
382 increases from 0 to 300 vehicles per kilometer and the results are shown in Fig. 14 and Fig. 15,
383 respectively. As can be seen from Fig. 14, there is a linear increasing trend of the expected number of
384 vehicles and persons as density of vehicles increases. When the density of vehicles is equal to 300
385 vehicles per kilometer, the expected number can reach 1.01×10^{-2} vehicles being hit per year and 5.52
386 $\times 10^{-2}$ persons being hit per year, respectively. As can be seen from Fig. 15, the societal risk also
387 increases as the density of vehicles becomes larger. When density of vehicles is less than 10 vehicles
388 per kilometer, the societal risk will be within the ALARP region. Therefore, depending on the density

of the vehicles, the societal risk of a landslide may be acceptable when it is located near one highway but become unacceptable when it is located at another highway. Therefore, in the design of highway slopes, the failure probability of the slope should be decreased as the density of the vehicles increases.

5 Limitations and Applicability of the Method Suggested in This Study

The rainfall condition may affect the failure probability of the slope as well as the traffic density and hence affect the risk. In this case study, the effect of rainfall condition on the annual failure probability of the slope is considered through Eq. (6), based on which both the chances of different types of rainfall as well as the failure probabilities of the slope under different types of rainfall are considered. The traffic condition may also vary with the rainfall condition. However, data on the impact of rainfall condition on the traffic density are rarely available. In this study, the impact of rainfall condition on the traffic flow is not considered in the risk assessment.

The method used for case study consists of three components, i.e., the hazard probability model, the spatial impact assessment model, and the consequence assessment model. The annual failure probability of the slope is calculated based on statistical analysis of past failure data in Hong Kong. It represents the failure probability of an average slope in Hong Kong, which is a common assumption adopted in empirical methods. When the method is applied in another region, the failure probability should be estimated using data from the region under study. Alternatively, to reflect the effects of factors like slope geometry and local ground conditions on slope failure probability, the failure probability can also be estimated using physically-based methods. As mentioned previously, current physically-based methods mainly focus the failure probability of a slope during a given rainfall event.

410 It is important to also examine how to incorporate the uncertainty of the rainfall condition into the
411 slope failure probability evaluation in future studies.

412 In this study, the spatial impact is estimated based on an empirical runout distance prediction
413 equation based on the data of different types of landslides from several countries. When applying the
414 method suggested in this paper in another region, the empirical equation should be tested that whether
415 it can better fit landslides in the region under study or one should estimate the runout distance based
416 on empirical relationships developed in the region under study. The spatial impact of the landslide may
417 also be estimated using physically-based models. In recent years, large deformation analysis methods
418 have been increasingly used for runout distance analysis. It should be noted that, during the runout
419 distance analysis, the uncertainties in the geological condition and soil properties should be considered.
420 Currently, the large deformation analysis is often carried out in a deterministic way. It is highly
421 desirable to combine the large deformation analysis with the reliability theory such that the spatial
422 impact of the landslide can also be predicted probabilistically.

423 The consequence assessment model is generally applicable and can be used assessment the impact
424 of landslides on moving vehicles in other regions. Therefore, after the hazard probability model and
425 the spatial impact model are replaced with models suitable for application in another region, the
426 suggested method in this paper can also be used for assessing the risk of moving vehicles hit by a
427 rainfall-induced landslide in another region.

428 There are multiple scenarios for a landslide to impact vehicles on the highway. The focus of this
429 paper is on the impact of falling materials on moving vehicles. In future studies, it is also worthwhile
430 to develop methods to evaluate the effect of uncertainty in the number and types of vehicles on risk
431 assessment of the impact of a landslide on vehicles in other scenarios.

6 Summary and Conclusions

When assessing the risk of landslide hitting the moving vehicles, the number and types of vehicles being hit could be highly uncertain. Using a case study in Hong Kong, this paper suggests a method to assess the risk of vehicles hit by a rainfall-induced landslide with explicit considering of the above factors. The research findings from this study can be summarized as follows.

(1) With the method suggested in this paper, the expected annual number of vehicles/persons hit by the landslide as well as the cumulative frequency-number of fatalities curve can be calculated. These results can provide important complement to those from previous studies on risk assessment of landslide hitting moving vehicles, which mainly focus on the individual risk of a landslide or societal risk assessment relying on the probability of the occurrence of at least one fatality per year.

(2) As the length, density, as well as the passage capacity of different vehicles are different, the annual number of vehicles/persons hit by the landslide for different types of vehicles are not the same. The societal risk associated with different types of vehicles are also different. It is important to consider different types of vehicles in the traffic flow.

(3) The suggested method can be used to examine the effect of factors like the annual failure probability of the slope and the density of the vehicles on the road on the risk of landslide hitting moving vehicles. The proposed method can be potentially useful to determine the target annual failure probability of a slope considering the traffic condition at a highway, which can be used as a new guideline for highway landslide risk management.

In this case study, the annual failure probability of the slope is evaluated based on a statistical model, and the spatial impact of the landslide is analyzed through an empirical equation. While these

methods are easy to use, they cannot consider the effect of local geology and soil condition on the failure and post-failure behavior of the slope. Further studies are needed to explore physically-based methods to predict the annual failure probability and runout distance with explicit consideration of the uncertainties involved.

Acknowledgements

This research was substantially supported by the National Key Research and Development Program of China (2018YFC0809600, 2018YFC0809601), the National Natural Science Foundation of China (41672276，51538009), the Key Innovation Team Program of MOST of China (2016RA4059), and Fundamental Research Funds for the Central Universities.

References

Bíl, M., Vodák, R., Kubeček, J., Bílová, M., and Sedoník, J.: Evaluating road network damage caused by natural disasters in the czech republic between 1997 and 2010, Transportation Research Part A, 80, 90–103, 2015.

Budetta, P., and Riso, R. D.: The mobility of some debris flows in pyroclastic deposits of the northwestern Campanian region (southern Italy), Bulletin of Engineering Geology and the Environment, 63, 293–302, 2004.

Bunce, C., Cruden, D., and Morgenstern, N.: Assessment of the hazard from rock fall on a highway, Canadian Geotechnical Journal, 34, 344–356, 1997.

Brand, E.W.: Landslides in Southeast Asia: A State-of-the-art Report, in: Proceedings of the 4th International Symposium on Landslides, Toronto, Vol. 1, pp. 17–59, 1984.

Budetta, P.: Assessment of rockfall risk along roads, Natural Hazards and Earth System Sciences, 4, 71-81, 2004.

478 Carter, M., and Bentley S. P.: The geometry of slip surfaces beneath landslides-predictions from
479 surface measurements, Canadian Geotechnical Journal, 22, 234–238, 1985.
480 Cascini, L., Ferlisi, S., and Vitolo, E.: Individual and societal risk owing to landslides in the Campania
481 region (southern Italy), Georisk, 2, 125–140, 2008.
482 Christian, J. T., Ladd, C. C., and Baecher, G. B.: Reliability applied to slope stability analysis, Journal
483 of Geotechnical Engineering, ASCE, 120, 2180–2207, 1994.
484 Chau, K. T., Sze, Y. L., Fung, M. K., Wong, W. Y., Fong, E. L., and Chan, L. C. P.: Landslide hazard
485 analysis for Hong Kong using landslide inventory and GIS, Computers and Geosciences, 30,
486 429–443, 2004.
487 Chen, H. X., and Zhang, L. M.: A physically-based distributed cell model for predicting regional
488 rainfall-induced shallow slope failures, Engineering Geology, 176, 79–92, 2014.
489 Cheung, R. W. M., and Tang, W. H.: Realistic assessment of slope reliability for effective landslide
490 hazard management, Geotechnique, 55, 85–94, 2005.
491 Corominas, J.: The angle of reach as a mobility index for small and large landslides, Canadian
492 Geotechnical Journal, 33, 260–271, 1996.
493 Corominas, J. and Mavrouli, O.: Rockfall quantitative risk assessment, in: Rockfall Engineering, edited
494 by: Lambert, S. and Nicot, F., John Wiley and Sons, Inc., Hoboken, 255–301, 2013.
495 Donnini, M., Napolitano, E., Salvati, P., Ardizzone, F., Bucci, F., and Fiorucci, F., et al.: Impact of
496 event landslides on road networks: a statistical analysis of two Italian case studies, Landslides, 14,
497 1–15, 2017.
498 Dai, F. C., Lee, C. F., and Ngai, Y. Y.: Landslide risk assessment and management: an overview,
499 Engineering Geology, 64, 65–87, 2002.
500 Dorren, L., Sandri, A., Raetzo, H., and Arnold, P.: Landslide risk mapping for the entire Swiss national
501 road network, in: Malet, J. P., Remaître, A., and Bogaard, T. (Eds.), Landslide Processes: From

502 Geomorphologic Mapping to Dynamic Modelling, Utrecht University and University of Strasbourg,
503 Strasbourg, pp. 6–7, 2009.
504 Dai, F., and Lee, C.: Landslide characteristics and slope instability modeling using GIS, Lantau Island,
505 Hong Kong, Geomorphology, 42, 213–228, 2002.
506 Erener, A.: A regional scale quantitative risk assessment for landslides: Case of kumluca watershed in
507 Bartin, Turkey, Landslides, 10, 55–73, 2012.
508 Fenton, G. A., and Griffiths, D. V.: A slope stability reliability model, in: Proceeding of the K.Y. Lo
509 Symposium (on CD), London, Ontario, July 7–8, 2005.
510 Finlay, P. J., and Fell, R.: Landslides: risk perception and acceptance, Canadian Geotechnical Journal,
511 34, 169–188, 1997.
512 Finlay, P. J., Mostyn, G. R., and Fell, R.: Landslide risk assessment: prediction of travel distance,
513 Canadian Geotechnical Journal, 36, 556–562, 1999.
514 Fell, R., Ho, K. K. S., Lacasse, S., and Leroi, E.: A framework for landslide risk assessment and
515 management, in: Hungr, O., Fell, R., Couture, R., and Eberhardt, E. (Eds.), Landslide Risk
516 Management, Taylor and Francis, London, pp. 3–26, 2005.
517 Fell, R.: Landslide risk assessment and acceptable risk, Canadian Geotechnical Journal, 31, 261–272,
518 1994.
519 Ferlisi, S., Cascini, L., Corominas, J., and Matano, F.: Rockfall risk assessment to persons travelling
520 in vehicles along a road: the case study of the Amalfi coastal road (southern Italy), Natural Hazards,
521 62, 691–721, 2012.
522 GovHK: Hong Kong–the Facts, Retrieved from www.gov.hk, 2019.
523 Gao, L., Zhang, L. M., and Chen, H. X.: Likely scenarios of natural terrain shallow slope failures on
524 Hong Kong Island under extreme storms, Natural Hazards Review, 18, B4015001, 2017.
525 Geotechnical Engineering Office (GEO): Highway slope manual, Civil Engineering and Development
526 Dept., Government of Hong Kong SAR, Hong Kong, 2017.

527 Geotechnical Engineering Office (GEO): Investigation of some major slope failures between 1992 and
528 1995, Civil Engineering and Development Dept., Government of Hong Kong SAR, Hong Kong,
529 1996.
530 Geotechnical Engineering Office (GEO): Landslides and boulder falls from natural terrain: interim risk
531 guidelines, GEO Report No. 75, Geotechnical Engineering Office, Government of the Hong Kong
532 Special Administrative Region, 1998.
533 Guzzetti, F., Ardizzone, F., Cardinali, M., Galli, M., Reichenbach, P., and Rossi, M.: Distribution of
534 landslides in the Upper Tiber River basin, central Italy, Geomorphology, 96, 105–122, 2008.
535 Guzzetti, F., Ardizzone, F., Cardinali, M., Rossi, M., and Valigi, D.: Landslide volumes and landslide
536 mobilization rates in Umbria, central Italy, Earth and Planetary Science Letters, 279, 0–229, 2009.
537 Hong Kong Observatory (HKO): Climate Statistics, Retrieved from www.hko.gov.hk, 2018.
538 Huang, J., Griffiths, D. V., and Fenton, G. A.: System reliability of slopes by RFEM, Soils and
539 Foundations, 50, 343–353, 2010.
540 Huang, J., Lyamin, A. V., Griffiths, D. V., Krabbenhoft, K., and Sloan, S. W.: Quantitative risk
541 assessment of landslide by limit analysis and random fields, Computers and Geotechnics, 53, 60–67,
542 2013.
543 Hosking, J. R. M., Wallis, J. R., and Wood, E. F.: Estimation of the generalized extreme-value
544 distribution by the method of probability-weighted moments, Technometrics, 27, 251–261, 1985.
545 Hungr, O., Evans, S. G., and Hazzard, J.: Magnitude and frequency of rock falls and rock slides along
546 the main transportation corridors of southwestern British Columbia, Canadian Geotechnical Journal,
547 36, 224–238, 1999.
548 Hungr, O., and McDougall, S.: Two numerical models for landslide dynamic analysis, Computers and
549 Geosciences, 35, 978–992, 2009.

Hungr, O., Corominas, J., and Eberhardt, E.: Estimating landslide motion mechanism, travel distance and velocity, in: Hungr, O., Fell, R., Couture, R., and Eberhardt, E. (Eds.), Landslide Risk Management, Taylor and Francis, London, pp. 99–128, 2005.

Imaizumi, F., and Sidle, R. C.: Linkage of sediment supply and transport processes in Miyagawa Dam catchment, Japan, Journal Geophysical Research, 112, F03012, 2007.

Jaboyedoff, M., Oppikofer, T., Abellán, A., Derron, M. H., Loye, A., Metzger, R., and Pedrazzini, A.: Use of LIDAR in landslide investigations: A review, Nature Hazards, 61, 5–28, 2012.

Jaboyedoff, M., Carrea, D., Derron, M. H., Oppikofer, T., Penna, I. M., and Rudaz, B.: A review of methods used to estimate failure surface depths and volumes, Engineering Geology, 267, 2020 (in press).

Lessing, P., Messina, C. P., and Fonner, R. F.: Landslide risk assessment. Environmental Geology, 5, 93–99, 1983.

Luo, H. Y., Zhang, L. L., and Zhang, L. M.: Progressive failure of buildings under landslide impact, Landslides, 16, 1327–1340, 2019.

Lighthill, M., J.: On kinematic waves ii. a theory of traffic flow on long crowded roads, Proceedings of the Royal Society, A Mathematical Physical & Engineering Sciences, 229, 317–345, 1955.

Lumb, P.: Slope failures in Hong Kong. Quarterly Journal of Geology, 8, 31–65, 1975.

Michoud, C., Derron, M. H., Horton, P., Jaboyedoff, M., Baillifard, F. J., Loye, A., Nicolet, P., Pedrazzini, A., and Queyrel, A.: Rockfall hazard and risk assessments along roads at a regional scale: example in Swiss Alps, Natural Hazards and Earth System Sciences, 12, 615–629, 2012.

Macciotta, R., Martin, D. C., Morgenstern, N. R., and Cruden, D. M.: Quantitative risk assessment of slope hazards along a section of railway in the Canadian Cordillera—a methodology considering the uncertainty in the results, Landslides, 13, 115–127, 2015.

Macciotta, R., Martin, D. C., Cruden, D. M., Hendry, M., and Edwards, T.: Rock fall hazard control along a section of railway based on quantified risk, Georisk, 11, 272–284, 2017.

575 Macciotta, R., Gräpel, C., Keegan, T., Duxbury, J., and Skirrow, R.: Quantitative risk assessment of
576 rock slope instabilities that threaten a highway near Canmore, Alberta, Canada: managing risk
577 calculation uncertainty in practice, Canadian Geotechnical Journal, 37, 1–17, 2019.
578 Malamud, B. D., Turcotte, D. L., Guzzetti, F., and Reichenbach, P.: Landslide inventories and their
579 statistical properties, Earth Surface Processes and Landforms, 29, 687–711, 2004.
580 Nicolet, P., Jaboyedoff, M., Cloutier, C., Crosta, G. B., and Lévy, S.: Brief communication: on direct
581 impact probability of landslides on vehicles, Natural Hazards and Earth System Sciences, 16,
582 995–1004, 2016.
583 Negi, I. S., Kumar, K., Kathait, A., and Prasad, P. S.: Cost assessment of losses due to recent
584 reactivation of Kaliasaur landslide on National Highway 58 in Garhwal Himalaya, Natural Hazards,
585 68, 901–914, 2013.
586 Paxson, V., and Floyd, S.: Wide-area traffic: The failure of Poisson modeling, IEEE/ACM Transactions
587 on Networking, 3, 226–244, 1995.
588 Parker, R. N., Densmore, A. L., Rosser, N. J., De Michele, M., Li, Y., and Huang, R., et al.: Mass
589 wasting triggered by the 2008 Wenchuan earthquake is greater than orogenic growth, Nature
590 Geoscience, 4, 449–452, 2011.
591 Peila, D., and Guardini, C.: Use of the event tree to assess the risk reduction obtained from rockfall
592 protection devices, Natural Hazards and Earth System Sciences, 8, 1441–1450, 2008.
593 Pierson, L. A.: Rockfall hazard rating system, in: Rockfall: Characterization and Control, edited by:
594 Turner, A. K. and Schuster, R. L., Trans Res Board, Washington, D.C., 2012.
595 Remondo, J., Bonachea, J., and Cendrero, A.: Quantitative landslide risk assessment and mapping on
596 the basis of recent occurrences, Geomorphology, 94, 496–507, 2008.
597 Scheidegger, A. E.: On the prediction of the reach and velocity of catastrophic landslides, Rock
598 Mechanics and Rock Engineering, 5, 231–236, 1973.

599 Transport Department of Hong Kong (TDHK): Transport in Hong Kong, Retrieved from
600 www.td.gov.hk, 2018.
601 Vega, J. A., and Hidalgo, C. A.: Quantitative risk assessment of landslides triggered by earthquakes
602 and rainfall based on direct costs of urban buildings, Geomorphology, 273, 217–235, 2016.
603 Zhang, J., and Tang, W. H.: Study of time-dependent reliability of old man-made slopes considering
604 model uncertainty, Georisk: Assessment and Management of Risk for Engineered Systems and
605 Geohazards, 3, 106–113, 2009.
606

List of Tables

List of Figures

637 Private buses, 2. Non-franchised public buses, 3. Franchised buses, 4. Taxis, 5. Private cars,
638 6. Public light buses, 7. Private light buses, 8. Goods vehicles, 9. Special purpose vehicles,
639 10. Government vehicles, 11. Motor cycles, 12. All types of vehicles)
640 **Figure 12.** Impact of annual failure probability of the slope on annual expected number of
641 elements being hit by the landslide
642 **Figure 13.** Impact of annual failure probability of the slope on annual societal risk
643 **Figure 14.** Impact of density of vehicles on annual expected number of elements being hit by the
644 landslide
645 **Figure 15.** Impact of density of vehicles on annual societal risk
646

647 Table 1. Percent, length and passenger capacity of vehicles in Hong Kong
648

Vehicles types	Percent (%)	Length (m)	Passenger capacity (persons)
Private buses	0.08	10	55
Non-franchised public buses	0.82	10	55
Franchised buses	0.72	10	55
Taxis	2.30	5	5
Private cars	71.41	5	5
Public light buses	0.50	9	33
Private light buses	0.39	9	33
Goods vehicles	13.77	12	2
Special purpose vehicles	0.23	5	1
Government vehicles	0.74	5	5
Motor cycles	9.24	2	1

649

650 Table 2. Number of vehicles passing a given cross section of road per hour and average speed of
651 vehicles on Kennedy Road in a day
652

Periods in a day	Morning peak (7–9 am)	Normal period	Evening peak (5–7 pm)
q (vehicles per hour)	3000	1500	2800
v (km per hour)	15	30	15

653

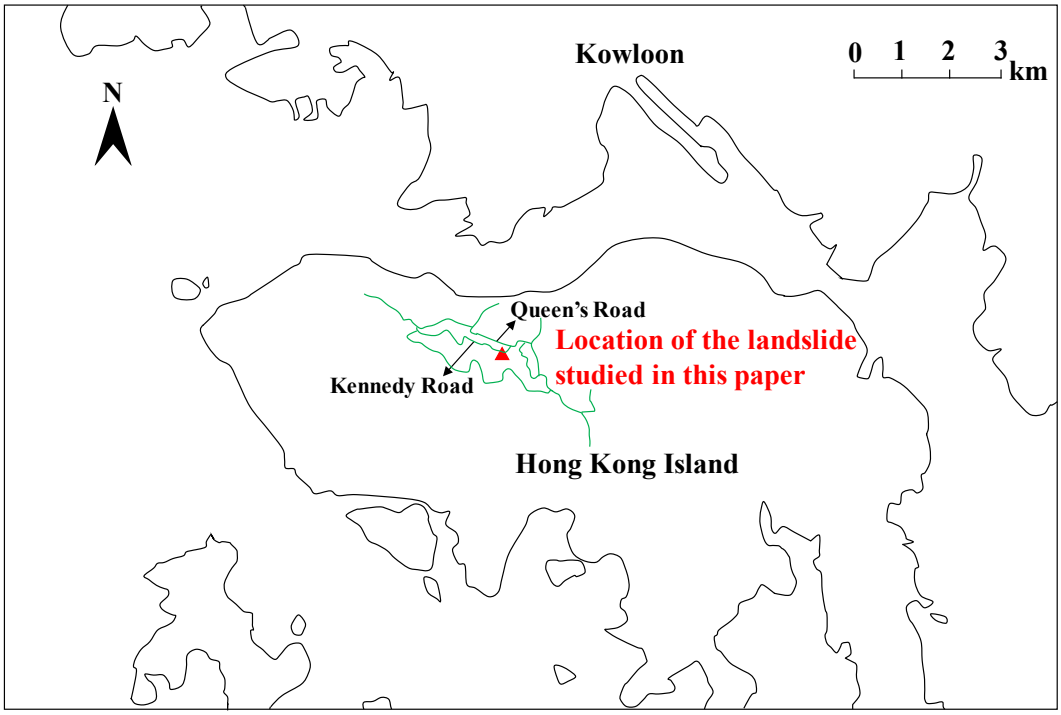

Figure 1. Location of the landslide studied in this paper

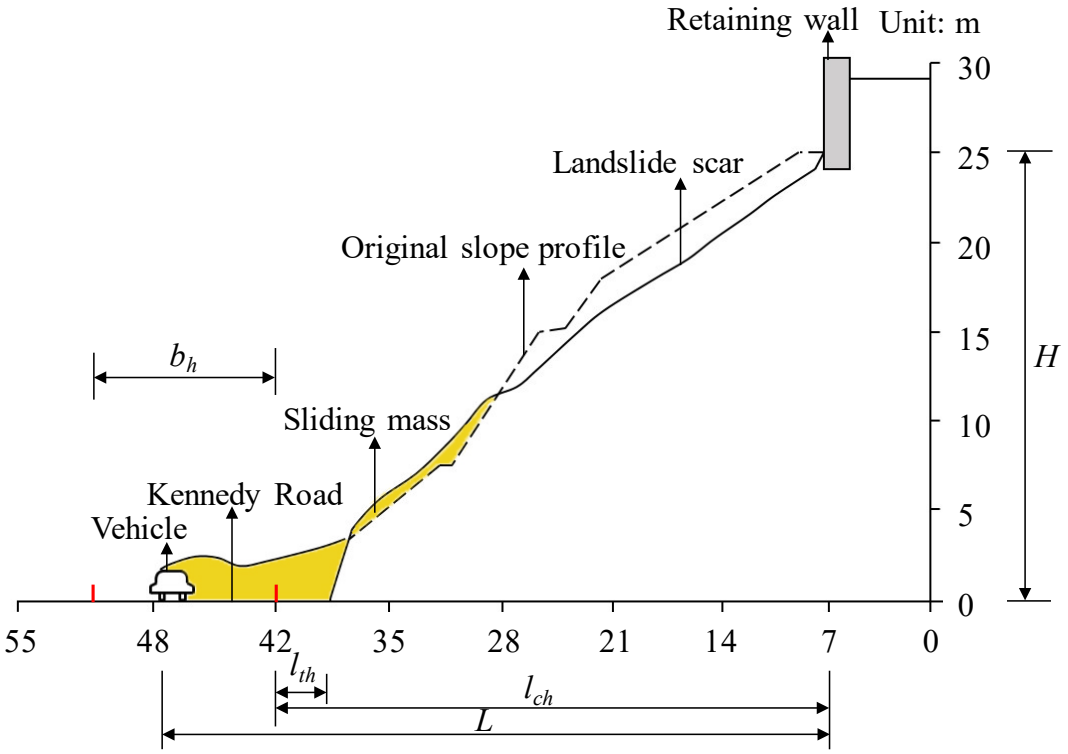

Figure 2. Typical cross section of the slope and the occurred landslide studied in this paper

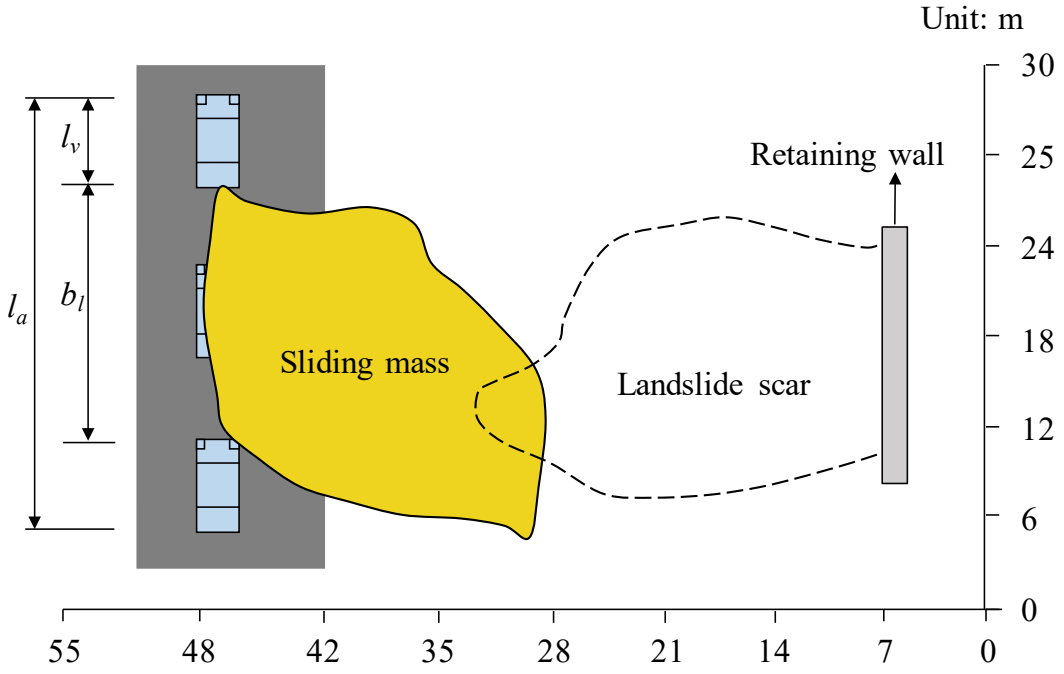

Figure 3. Plan view of the occurred landslide studied in this paper

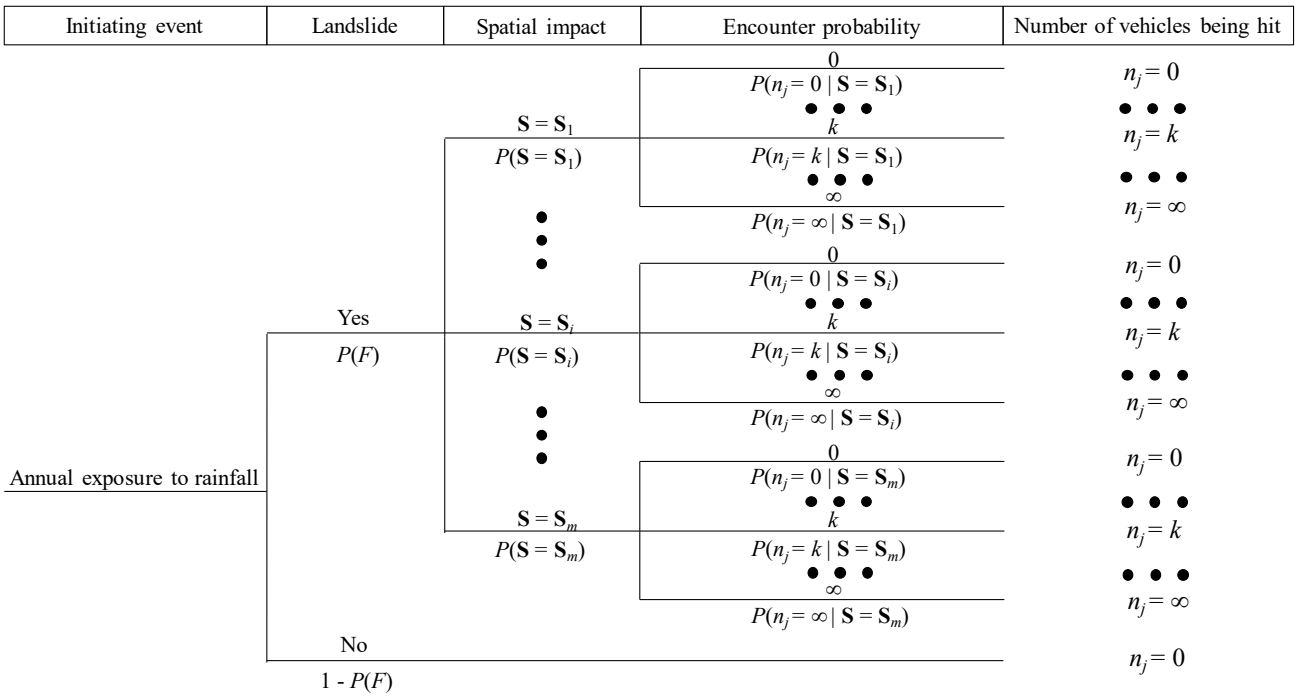

Figure 4. Event tree of evaluating the annual risk of the type *j* vehicle hit by the landslide

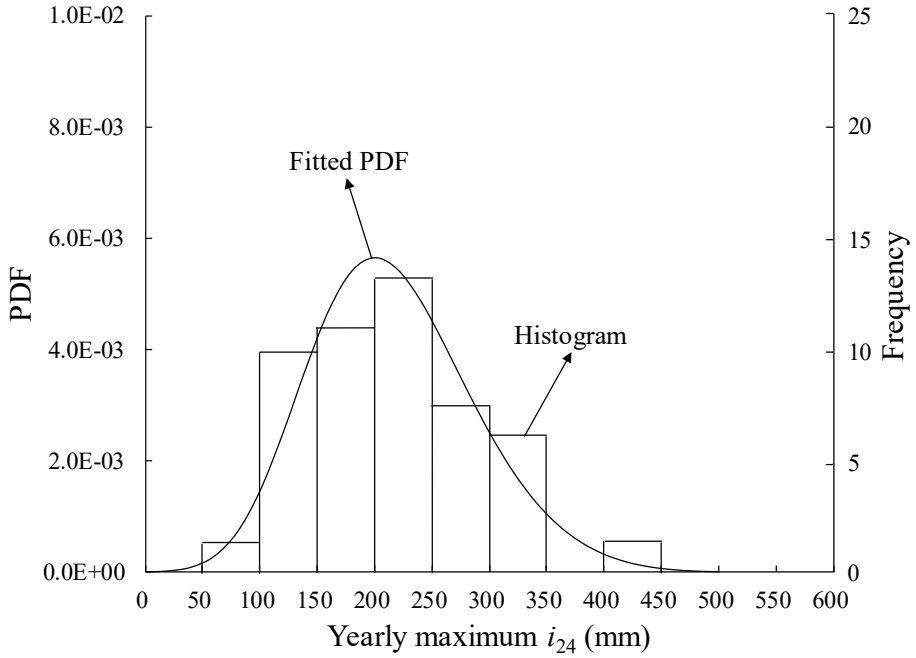

669
670

671 Figure 5. Histogram and fitted PDF of yearly maximum i_{24} in Hong Kong

672

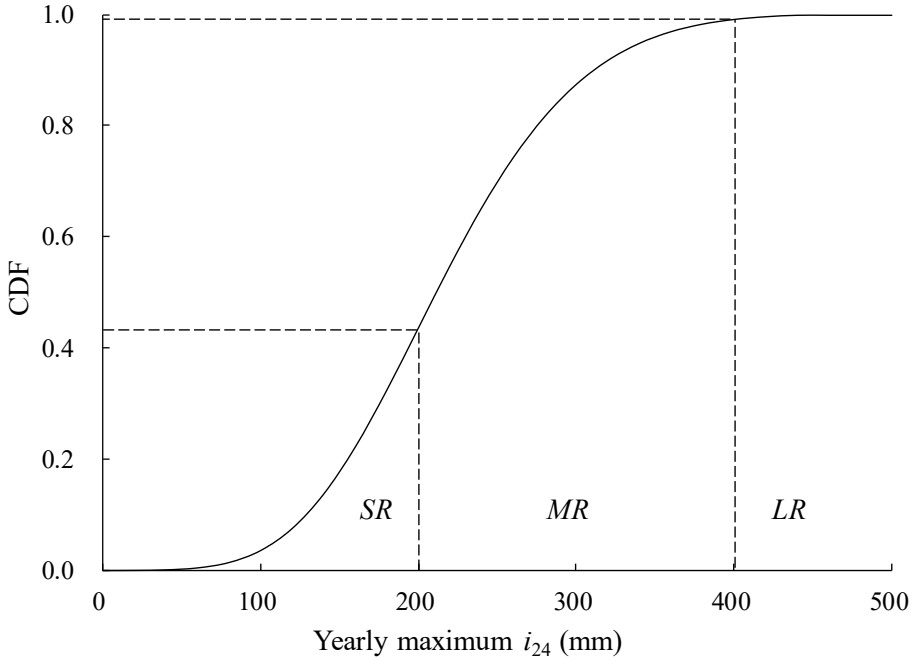

673
674

675 Figure 6. CDF of yearly maximum i_{24} in Hong Kong

676

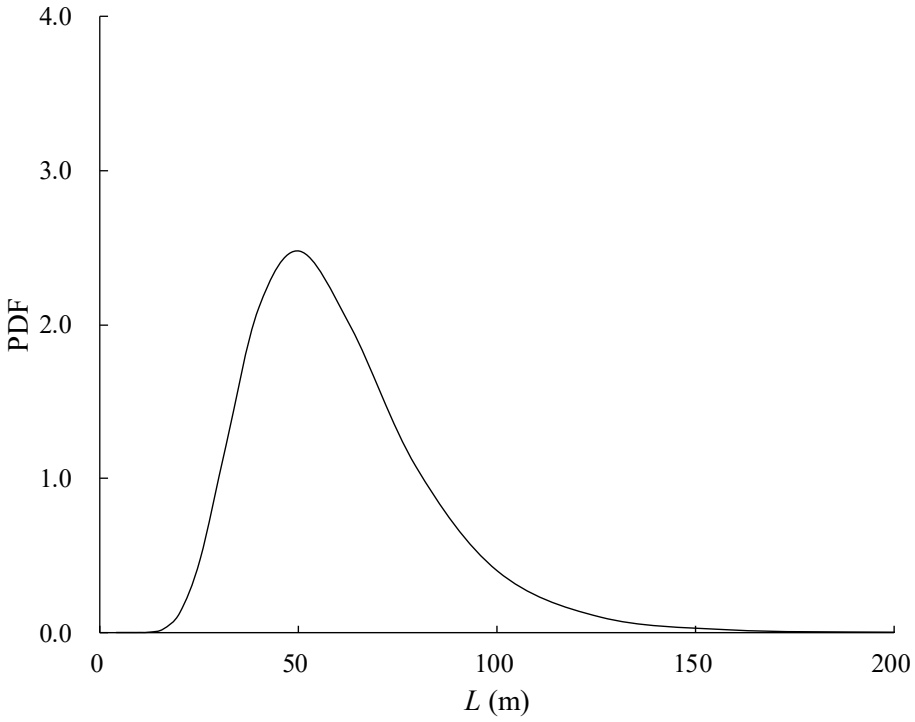

Figure 7. PDF of travel distance of the landslide studied in this paper

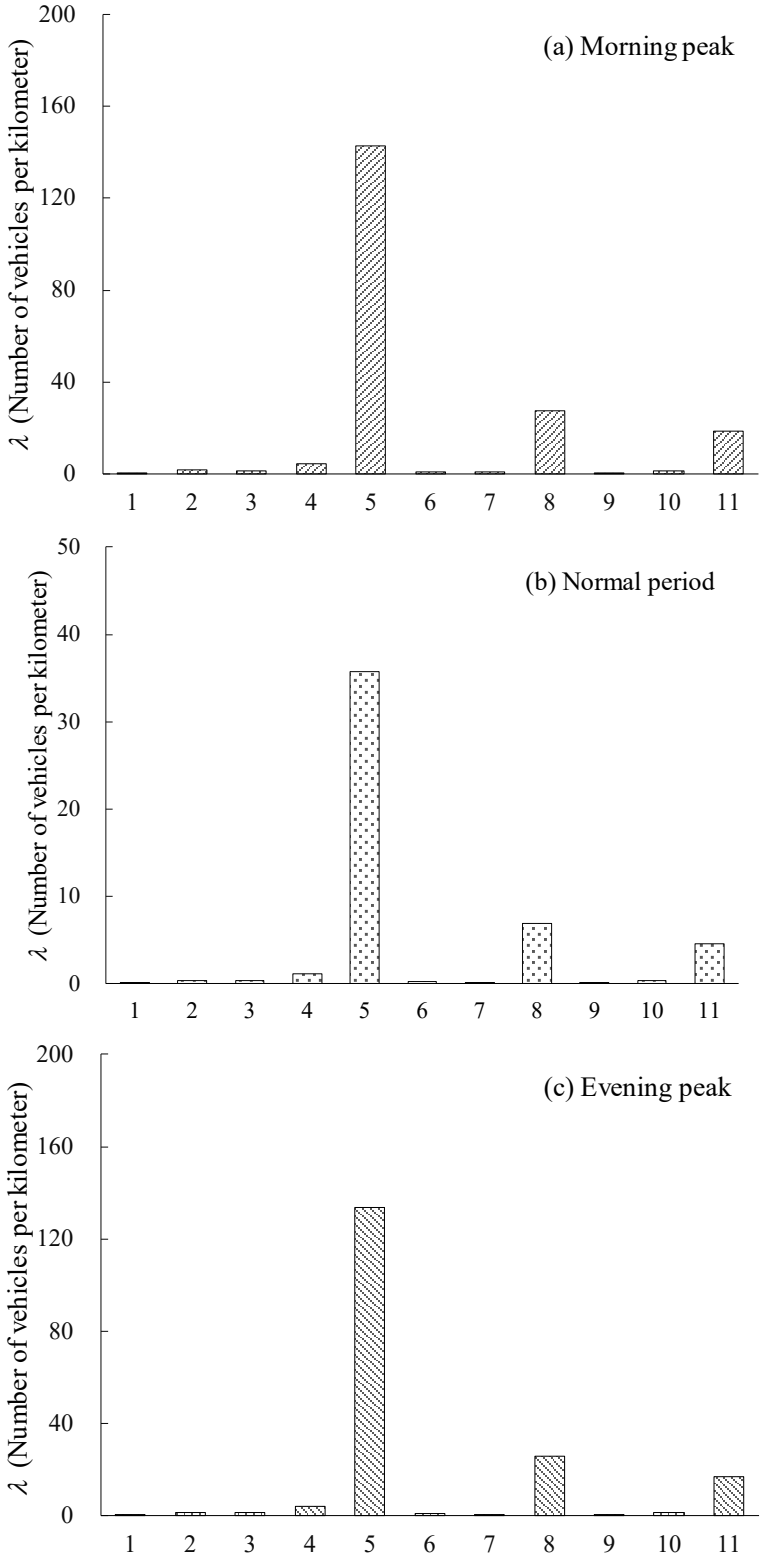

681

682

683

684

685 Figure 8. Mean rates of different types of vehicles during different periods: (a) morning peak (b)
686 normal period (c) evening peak. (1. Private buses, 2. Non-franchised public buses, 3. Franchised buses,
687 4. Taxis, 5. Private cars, 6. Public light buses, 7. Private light buses, 8. Goods vehicles, 9. Special
688 purpose vehicles, 10. Government vehicles, 11. Motor cycles)

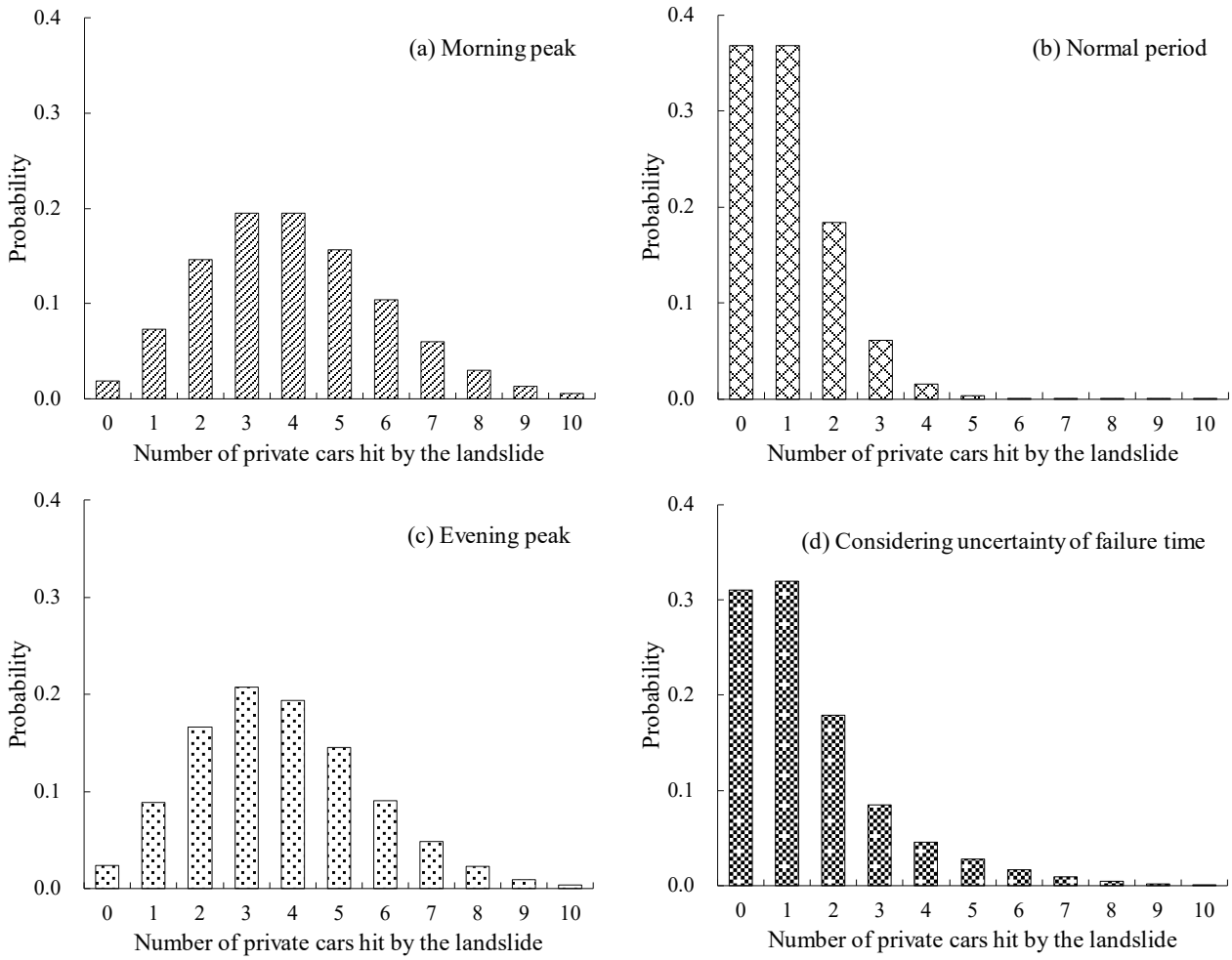

689

690 Figure 9. Probability distribution of number of private cars being hit by the landslide studied in this
691 paper during different periods when the spatial impact is $\mathbf{S}_i$ and $\alpha_j(\mathbf{S} = \mathbf{S}_i) = 1$: (a) morning peak, (b)
692 normal period, (c) evening peak, (d) considering uncertainty of failure time

693

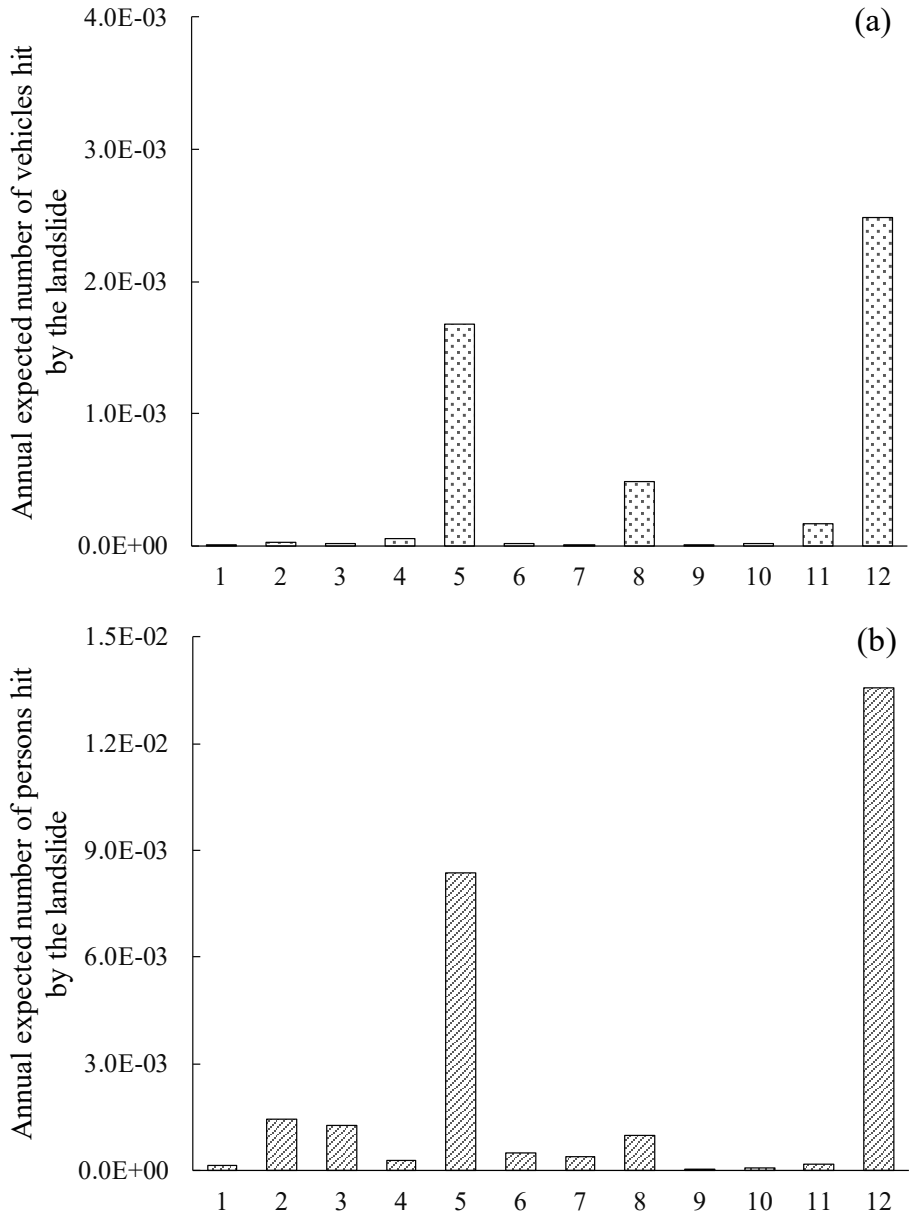

Figure 10. Annual expected number of elements being hit by the landslide studied in this paper: (a) vehicles (b) persons. (1. Private buses, 2. Non-franchised public buses, 3. Franchised buses, 4. Taxis, 5. Private cars, 6. Public light buses, 7. Private light buses, 8. Goods vehicles, 9. Special purpose vehicles, 10. Government vehicles, 11. Motor cycles, 12. All types of vehicles)

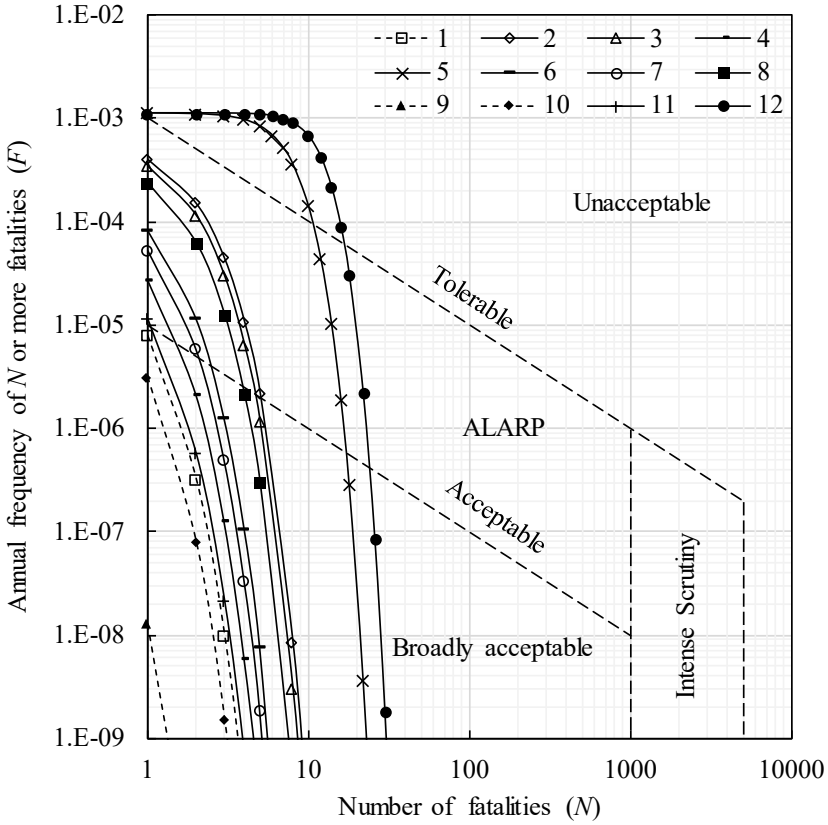

Figure 11. Estimated annual frequency of *N* or more persons being hit by the landslide studied in this paper (Tolerable and acceptable F-N curves are those specified by the GEO 1998). (1. Private buses, 2. Non-franchised public buses, 3. Franchised buses, 4. Taxis, 5. Private cars, 6. Public light buses, 7. Private light buses, 8. Goods vehicles, 9. Special purpose vehicles, 10. Government vehicles, 11. Motor cycles, 12. All types of vehicles)

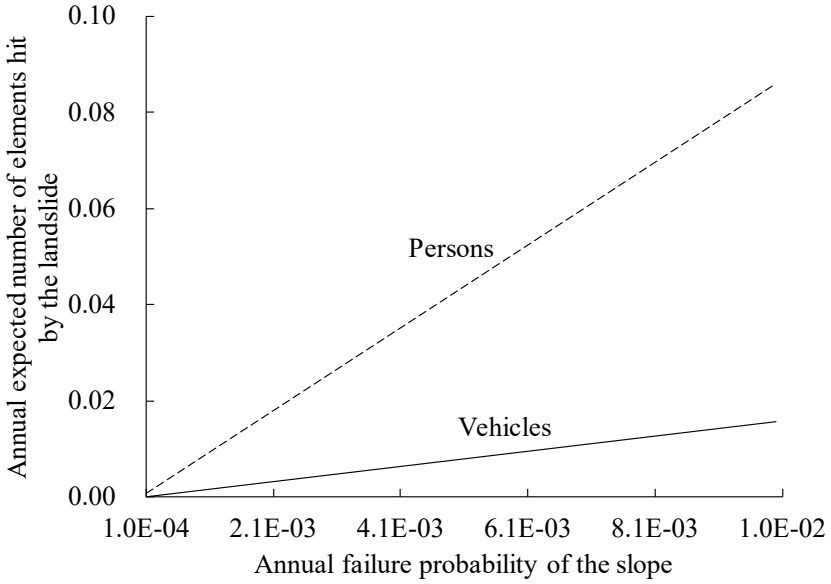

709

710 Figure 12. Impact of annual failure probability of the slope on annual expected number of elements
711 being hit by the landslide
712

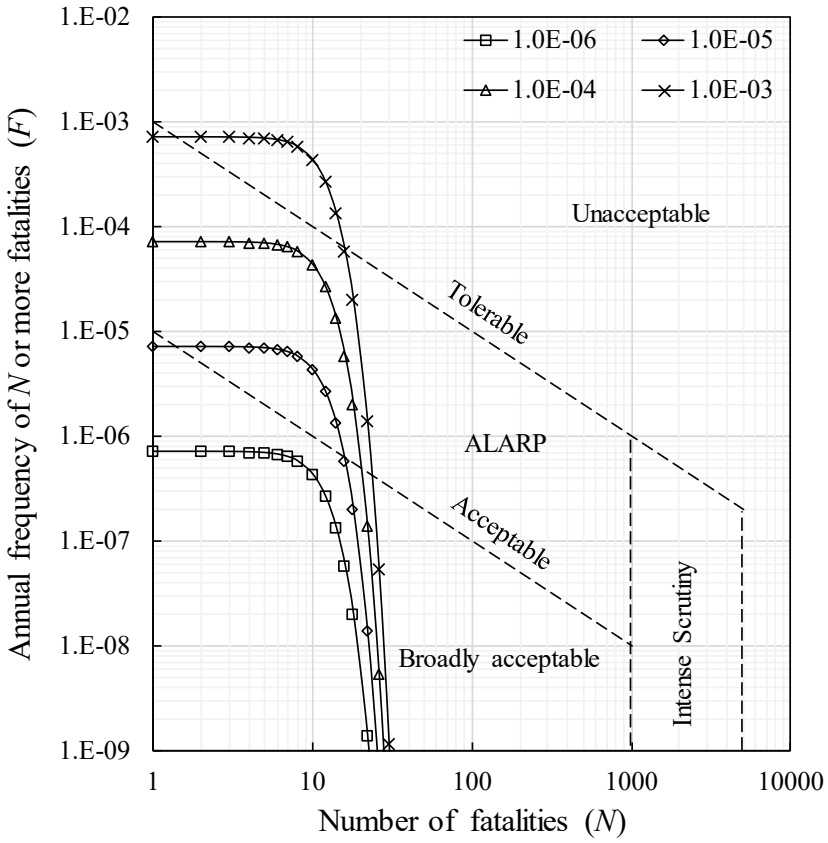

713

714 Figure 13. Impact of annual failure probability of the slope on annual societal risk

715

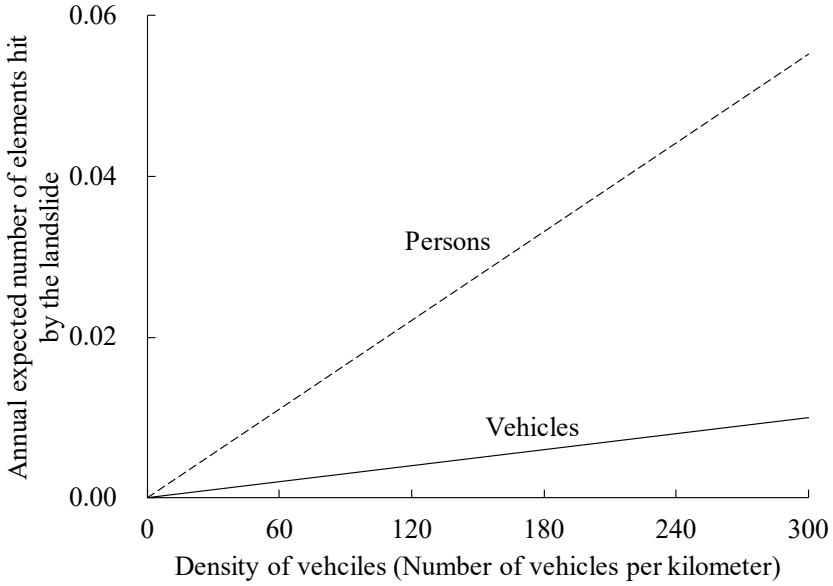

716

717 Figure 14. Impact of density of vehicles on annual expected number of elements being hit by the
718 landslide

719

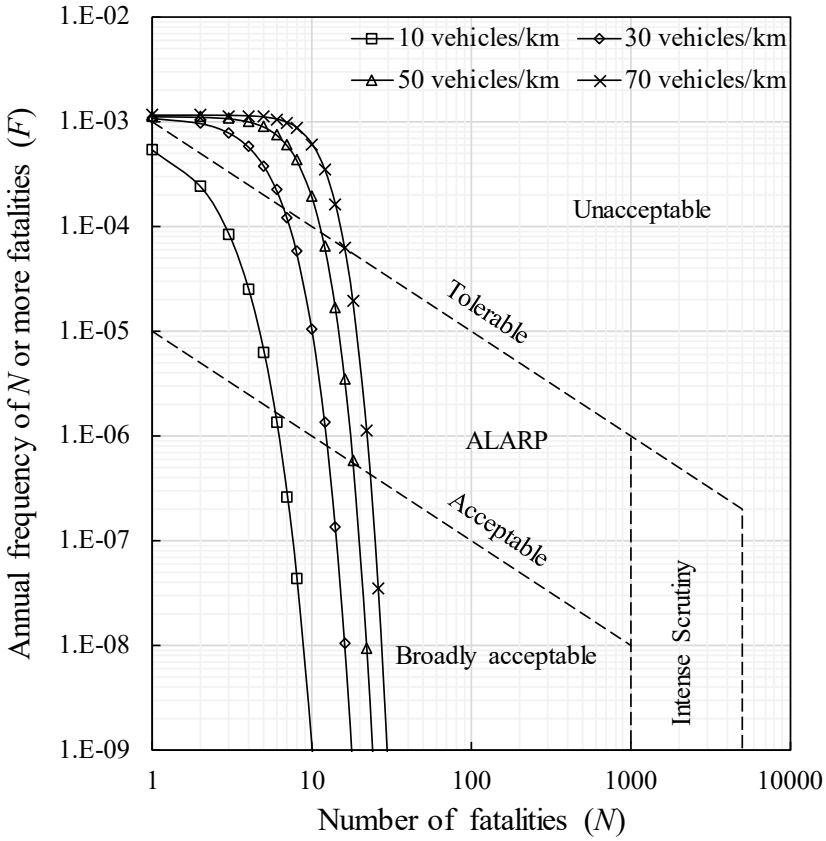

Figure 15. Impact of density of vehicles on annual societal risk